CFD-based Analysis & Correlation Development for a Novel Multi-furcating Heat Exchanger for High Temperature, High Pressure Applications

James Tancabel
University of Maryland, jmtanc@umd.edu

William Gerstler
General Electric Research Center

Daniel Erno

Jiazhen Ling

Vikrant Aute

Authors
James Tancabel, William Gerstler, Daniel Erno, Jiazhen Ling, Vikrant Aute, H Peter J. De Bock, and Reinhard Radermacher

CFD-based Analysis & Correlation Development for a Novel Multi-furcating Heat Exchanger for High Temperature, High Pressure Applications

James TANCABEL[1], William GERSTLER[2], Daniel ERNO[3], Jiazhen LING[4],
Vikrant AUTE[5]*, H. Peter J. DE BOCK[6], Reinhard RADERMACHER[7]

[1,4,5,7]Center for Environmental Energy Engineering
Department of Mechanical Engineering, University of Maryland
College Park, MD 20742 USA
Email: [1]jmtanc@umd.edu, [4]jiazhen@umd.edu, [5]vikrant@umd.edu, [7]raderm@umd.edu

[2,3,6]General Electric Research Center
Niskayuna, NY 12309 USA
Email: [2]gerstler@ge.com, [3]erno@ge.com, [6]debock@ research.ge.com

* Corresponding Author

ABSTRACT

The thermal efficiency of indirectly heated power cycles such as supercritical carbon dioxide (sCO_2) closed Brayton cycles are typically limited by their heat exchangers (HXs), which require high heat transfer effectiveness while operating for tens of thousands of hours under high temperature (>800°C) and pressure (>80 bar) conditions. Previous literature has shown that the use of nature-inspired furcating flow channels represents an exciting opportunity to improve HX thermal-hydraulic performance. In this paper, we analyze the novel multi-furcating HX manifold concept, that was previously shown experimentally to reduce HX volume and mass compared to a baseline oil cooler by 50% and 67%, respectively. Computational fluid dynamics (CFD) simulations are utilized to analyze thermal-hydraulic performance and fluid flow development. CFD-based correlations of Nusselt number and friction factor are developed for performance prediction of a full, additively manufactured HX. The developed Nusselt number and friction factor correlations predict unit cell thermal-hydraulic performance within ±3% and ±5% for all simulated Reynolds numbers, respectively. The full HX would enable increased thermal efficiency of indirectly heated power cycles to reduce both energy consumption and emissions while also allowing opportunities in advanced aerospace applications.

1. INTRODUCTION

In recent years, researchers have dedicated significant resources to developing environmentally-friendly, high efficiency power generation cycles to combat ever-increasing energy demands. In particular, indirect heating cycles such as supercritical carbon dioxide (sCO_2) closed Brayton cycles have gained traction due to their simple configuration, compact components, and superior thermal efficiency compared to high temperature two-phase power cycles (Dostal, 2004). Such traits make sCO_2 Brayton cycles particularly attractive for nuclear, waste heat recovery, solar thermal, supercritical cooling, and advanced aerospace applications (Serrano et al., 2014; Ahn et al., 2015; Cabeza et al., 2017; De Bock and Gerstler, 2019).

However, the thermal efficiency of sCO_2 systems is typically limited by the pressure and temperature capability of their heat exchangers (HXs), which must have high effectiveness while operating at high temperatures (>800°C) and pressures (>80 bar) for tens of thousands of hours during their lifetime. Classically, shell and tube HXs (STHXs) were utilized for such tasks; however, STHXs require tubes with large thicknesses to guarantee structural strength, resulting in large system footprints (Dostal, 2004; Serrano et al., 2014). More recently, printed circuit HXs have gained traction for sCO_2 applications due to their compactness and high temperatures and pressure capability, resulting in overall smaller systems while maintaining or improving cycle performance (Nitkin et al., 2006; Le Pierres et al., 2011; Serrano et al., 2014; Ahn et al., 2015; Meshram et al., 2016). Further, advancements in additive manufacturing (AM) and computational tools such as Computational Fluid Dynamics (CFD), Finite Element Analysis (FEA), and optimization algorithms have enabled engineers to design, prototype, and test HXs mimicking the characteristic high heat transfer and low flow resistance capabilities of fractal and furcating geometries found in nature (e.g., respiratory, vascular systems) (Huang et al., 2017).

Recently, Cabeza et al. (2017) presented a comprehensive review of all experimental studies and heat transfer correlations for sCO_2 flowing in a variety of flow channels and configurations. The review suggests a lack of published studies which simultaneously explore the high temperature and pressure conditions exhibited in the cycles of interest. Additionally, the authors concluded that no universal correlation exists for any single geometry, further emphasizing the need for comprehensive modeling and experimentation of novel HX geometries utilizing sCO_2.

In this paper, we analyze a previously developed novel multi-furcating HX manifold concept enabled by AM (Gerstler et al., 2016; Gerstler et al., 2017; Gerstler and Erno, 2017) which, when compared to a baseline oil cooler, has the potential to reduce HX volume and mass by 50% and 67%, respectively. CFD simulations are utilized to analyze the fluid flow and develop Nusselt number and friction factor correlations for performance prediction of a full, additively manufactured HX which can increase thermal efficiency of indirect heated power cycles to reduce both energy consumption and emissions while also allowing for opportunities in advanced aerospace applications.

2. METHODOLOGY

In this paper, we leverage CFD to evaluate the thermal-hydraulic performance (Nusselt number and friction factor) for a single unit cell of a multi-furcating HX manifold concept (Gerstler et al., 2016; Gerstler et al., 2017; Gerstler and Erno, 2017) (Figure 1). The framework consists of four steps: (i) problem specification, (ii) CFD modeling, (iii) correlation development, and (iv) correlation verification (Figure 2).

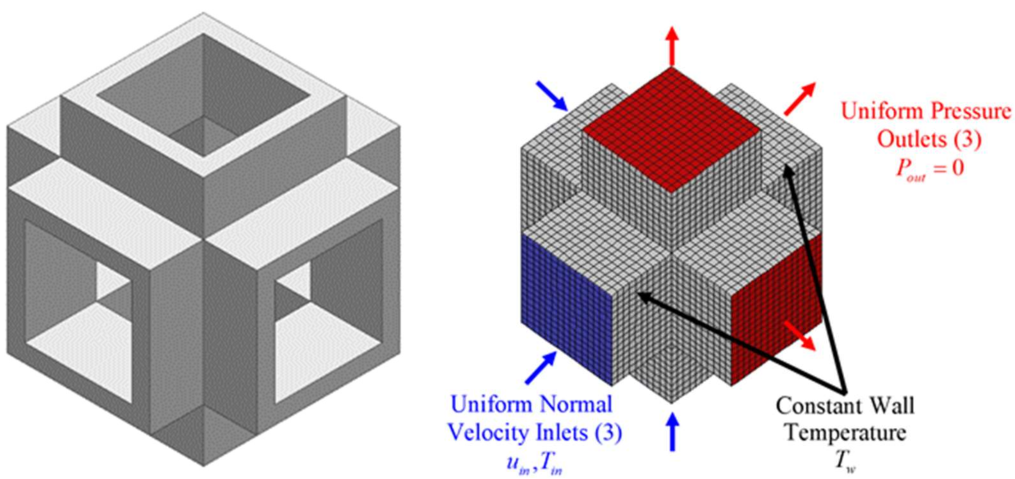

Figure 1: Unit cell geometry and computational domain (not to scale).

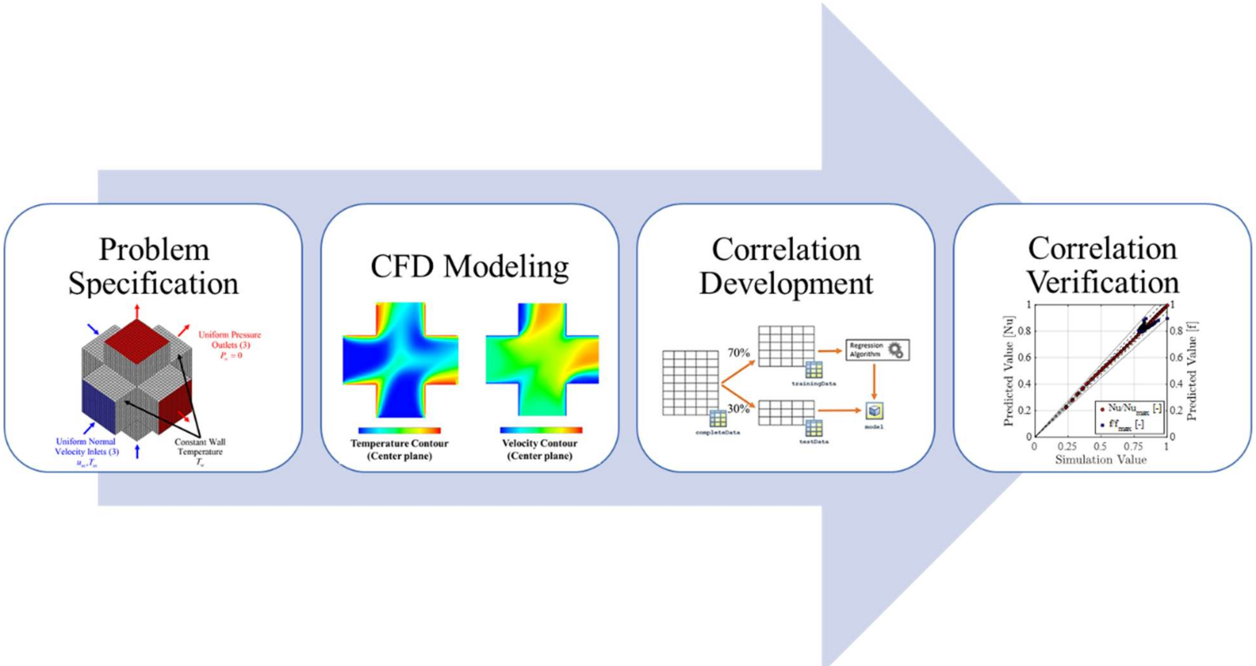

Figure 2: Correlation development flowchart.

3. PROBLEM SPECIFICATION

This paper investigates the thermal-hydraulic performance of a single unit cell of a previously developed novel multi-furcating HX manifold concept (Gerstler et al., 2016; Gerstler et al., 2017; Gerstler and Erno, 2017). The working fluids are air and sCO_2, which are studied individually. The thermal-hydraulic performance is approximated across an applicable range of Reynolds numbers at the representative temperature and pressure design points indicated in Table 1 (Private communications, 2019). Note that the sCO_2 operating condition is far from the critical point (304.13 K; 7.3773 MPa) (Span and Wagner, 1996).

Table 1: Design conditions (Private communications, 2019).

Working Fluid	Inlet Re [-]	T_{in} [K]	T_w [K]	Operating Pressure [MPa]
Air	100 – 1600	1173.15	1043.15	8.0
sCO_2		1043.15	1173.15	25.0

4. CFD MODELING AND SIMULATION

4.1 CFD Model Development

The CFD computational domain is a single, three-dimensional, multi-furcating unit cell with one fluid domain (Figure 1). The computational domain is meshed using an all-hex scheme with constant element size. The inlet boundary is a uniform velocity and temperature condition, and the outlet boundary is held constant at the operating pressure. The uniform velocity is computed from inlet Reynolds number for fair comparison across both fluids (see Table 1). All walls are set to a constant wall temperature equal to the operating temperature of the other fluid. By ignoring the thermal resistances of the other fluid and the wall, it is possible to evaluate the thermal-hydraulic performance of a single unit cell by itself. Turbulence is modeled using the k-ε realizable model (Shih et al., 1994), and the convergence criteria is set to 1E-05 for continuity and momentum, 1E-06 for energy, and 1E-03 for turbulence. All meshing is conducted in Ansys® R18.0 Mechanical (ANSYS, Inc., 2018a), and all CFD simulations are conducted using Ansys® Fluent R18.0 (ANSYS, Inc., 2018b).

4.1.1 Fluid Property Calculation: With the exception of air density, which is computed using the ideal gas model, the thermophysical properties for air and sCO_2 are computed as polynomial functions of temperature (Equation (1)).

$$\phi(T)=\sum_{i=1}^{N}A_i\cdot T^{i-1} \tag{1}$$

The polynomials are built from data obtained using NIST REFPROP Version 9.1 (Lemmon et al., 2013) for the operating ranges as described in Table 1 (Private communications, 2019). Table 2 lists the order of the polynomials used for thermophysical property calculation. Since air density is computed using the ideal gas model, that particular value of N is presented as "N/A". All property curve fits predict thermophysical properties within ±1% when compared to REFPROP across the entire operating range.

Table 2: Thermophysical property polynomial orders.

Air Property	**N [-]**	**sCO_2 Property**	**N [-]**
Density	N/A [Ideal Gas Model]	Density	3
Specific Heat	5	Specific Heat	5
Thermal Conductivity	3	Thermal Conductivity	3
Dynamic Viscosity	3	Dynamic Viscosity	3

4.2 Data Reduction

CFD models are utilized to compute the thermal-hydraulic performance of a single unit cell. It is not necessary to consider the thermal resistance of the wall and other fluid. Thus, the heat transfer coefficient can be evaluated using the UA-LMTD method (Equation (2)) (Bergman et al., 2011). Pressure drop is computed as the difference between the inlet and outlet static pressure, assuming the local losses to be negligible (Equation (3)).

$$\dot{Q}=\dot{m}c_p\Delta T=hA\Delta T_{LM}\Rightarrow h=\frac{\dot{m}c_{p,T_{avg}}}{A}\cdot\ln\left(\frac{T_{in}-T_w}{T_{out}-T_w}\right) \tag{2}$$

$$\Delta P=P_{in}-P_{out} \tag{3}$$

5. CORRELATION DEVELOPMENT

We propose correlations for Nusselt number and friction factor (Equations (4) and (5), respectively). Nondimensionalization occurs for fluid properties at temperature equal to the average of inlet and outlet fluid temperature and pressure equal to the fluid's operating pressure. Hydraulic diameter is computed as in Equation (6).

$$Nu=\frac{hD_h}{k_{T_{avg}}} \tag{4}$$

$$f=\frac{\Delta P}{\frac{1}{2}\rho_{T_{avg}}u^2}\cdot\frac{D_h}{L} \tag{5}$$

$$D_h=\frac{4\cdot V}{A} \tag{6}$$

The general Nusselt number correlation form is assumed to be a Dittus-Boelter-like equation (Equation (7)) (Dittus and Boelter, 1930), while friction factor form is assumed to be a power-law function of Reynolds number only (Equation (8)). The unknown coefficients X_1, X_2, X_3, Y_1, Y_2 are evaluated by conducting multiple linear regression on logarithmic transformations of Equations (7) and (8) (Equations (9) – (10)).

$$Nu = X_1 \cdot \mathrm{Re}^{X_2} \cdot \mathrm{Pr}^{X_3} \tag{7}$$

$$f = Y_1 \cdot \mathrm{Re}^{Y_2} \tag{8}$$

$$\ln(Nu) = \ln(X_1) + X_2 \cdot \ln(\mathrm{Re}) + X_3 \cdot \ln(\mathrm{Pr}) \tag{9}$$

$$\ln(f) = \ln(Y_1) + Y_2 \cdot \ln(\mathrm{Re}) \tag{10}$$

5.1 Correlation verification

To conduct model verification without running additional time-consuming 3D CFD simulations, the CFD data is divided into two sets: (i) a training set, consisting of 70% of the data, and (ii) a test set comprising the remaining 30% of data. The correlation is built using the training data, and the model is verified by comparing the predicted performance of the test data to actual CFD simulations at the test data conditions (see Figure 3). The correlation fitness is shown in Table 3, and a verification plot with error lines at ±2% and ±5% is shown in Figure 4. It is clear that new correlations predict all Nusselt number and friction factor test data within ±3% and ±5%, respectively.

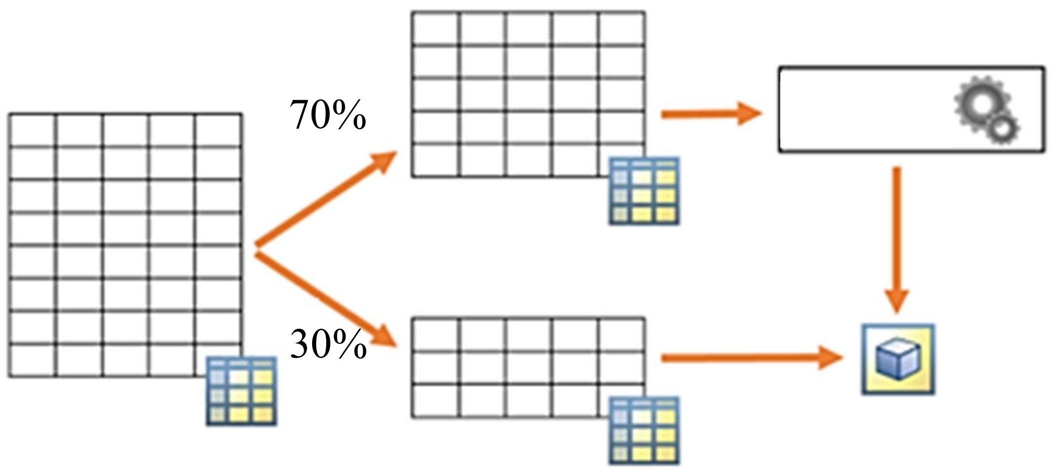

Figure 3: Correlation development schematic.

Table 3: Correlation fitness.

Metric	Nu	f
Predicted data (within ±2.0%)	94.74%	52.63%
Predicted data (within ±3.0%)	100%	78.95%
Predicted data (within ±4.0%)	100%	94.74%
Predicted data (within ±5.0%)	100%	100%
R^2	0.9988	0.4358
Mean Absolute Relative Error	0.533%	2.116%
Median Absolute Relative Error	0.398%	1.758%

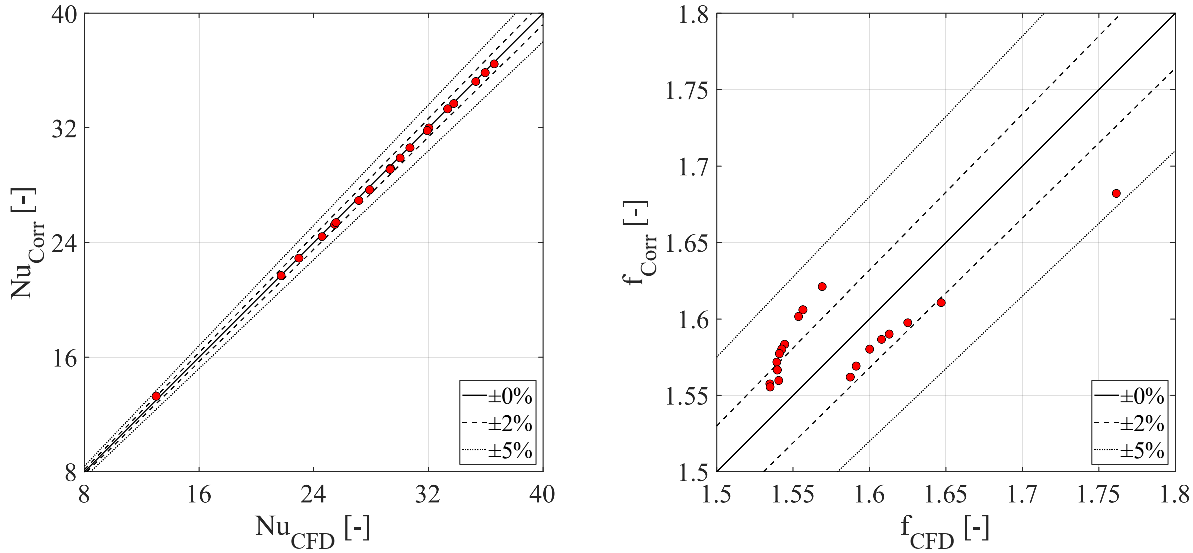

Figure 4: Unit cell correlation verification.

6. DISCUSSION

As noted by Cabeza et al. (2017), there exists no universal correlations to predict thermal-hydraulic performance sCO_2 HXs. To this end, we compare the proposed Nusselt number correlation to the Dittus-Boelter correlation (Dittus and Boelter, 1930), the theoretical fully developed laminar flow Nusselt number for uniform temperature (3.66) and heat flux (4.36) boundary conditions, and the laminar entry region Nusselt number for a HX with similar D_h/L as this unit cell (Bergman et al., 2011). The friction factor correlation is compared to the fully-developed laminar flow correlation and the Blasius correlation (Bergman et al., 2011).

Figure 5 shows the results of this analysis. It is clear that, though the unit cell flow is within the conventional laminar flow region ($Re < 2300$), neither the Nusselt number nor friction factor can be accurately modeled using laminar flow assumptions or other correlations from the literature. The new geometry's high Nusselt number is a direct function of the geometry itself: the furcating geometry has frequent thermal boundary layer resetting, which improves heat transfer (Gerstler and Erno, 2017). The proposed friction factor correlation utilizes a length scale unique to this geometry, so no true comparison can be conducted regarding the actual friction factor values. However, so long as the proper unit cell length scale is applied, the correlation is valid.

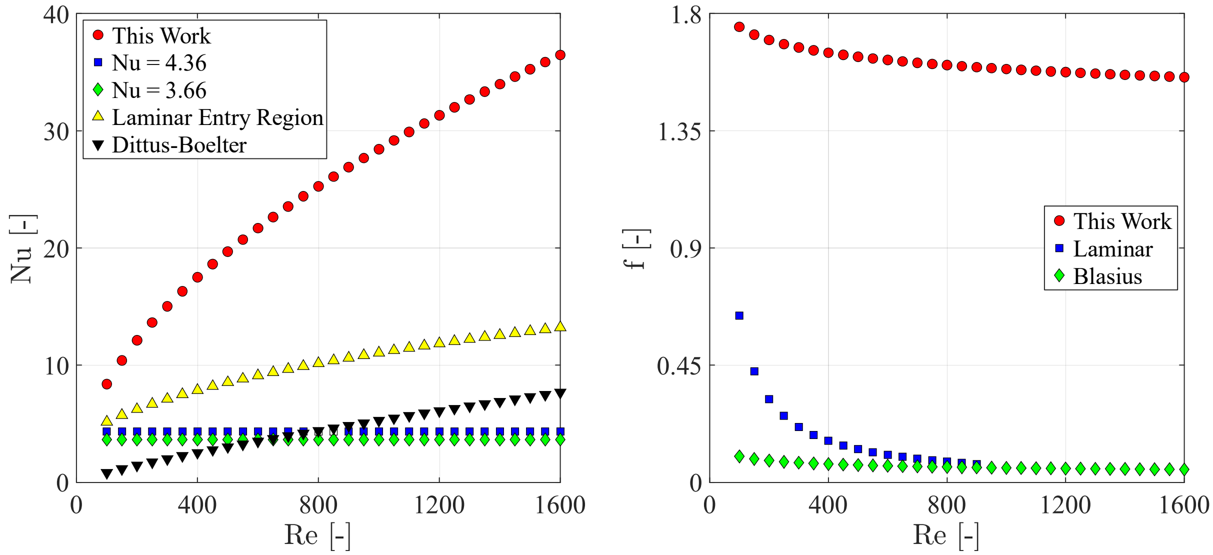

Figure 5: Unit cell correlation prediction compared to classic correlations.

Figure 6 below shows a comparison of this unit cell against some representative plate-fin surfaces with offset strip fins (Manglik and Bergles, 1995). The Webb efficiency (Webb and Kim, 2005) is utilized as the performance evaluation criteria (PEC) (Equation (11)). Again, the thermal-hydraulic benefits of the multi-furcating geometry compared to the plate fin HXs across the Reynolds number range is obvious.

$$\eta = \frac{Nu}{f^{1/3}} \tag{11}$$

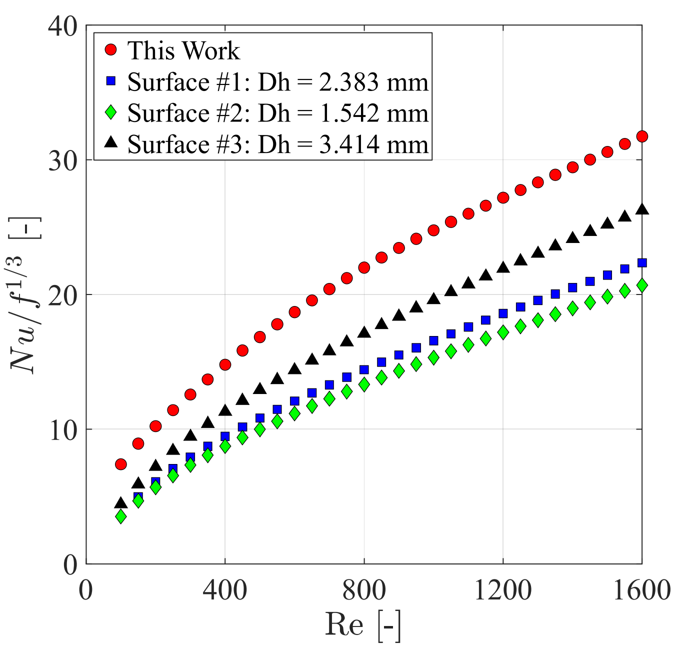

Figure 6: Web efficiency comparison: Unit cell versus plate-offset strip fin surfaces (Manglik and Bergles, 1995).

6.1 Flow development

It is of interest to better understand the flow development within a unit cell to explore how cells would interact in a full manifold. Figure 7 shows flow contours of temperature, velocity, and pressure taken at the center plane of a unit cell face for Re ≈ 150. Note how the flow furcation allows for boundary layer redevelopment and increased overall heat transfer (Gerstler and Erno, 2017). Additionally, the furcation acts as a "pseudo-contraction", increasing the flow velocity and thus heat transfer within the cell.

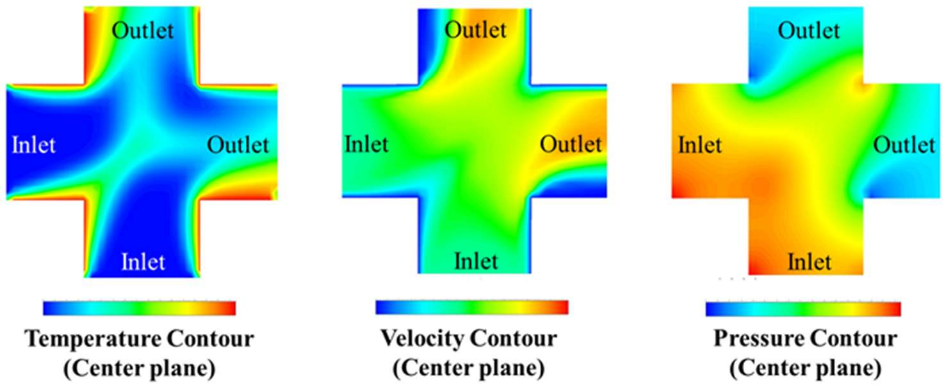

Figure 7: Unit cell flow contours of (Left) temperature, (Middle) velocity, and (Right) pressure (Re ≈ 150)

7. CONCLUSIONS

This paper presents an analysis of a unit cell novel multi-furcating HX manifold concept enabled by advancements in additive manufacturing technology. CFD is utilized to analyze the flow development within the unit cell and build correlations to predict the Nusselt number and friction factor. The developed correlations predict unit cell Nusselt number and friction factor within ±3% and ±5%, respectively. Additionally, we show how this HX unit cell concept cannot be modeled using conventional correlations, thus justifying the need for this analysis. The correlations will be utilized to predict the performance of a full-size additively manufactured HX, which can increase the thermal efficiency of indirectly heated power cycles while also allowing opportunities in advanced aerospace applications.

NOMENCLATURE

A	Unit cell surface area	(m²)	T	Temperature	(K)
c_p	Specific heat	(J/kgK)	u	Fluid velocity	(m/s)
D_h	Hydraulic diameter	(m)	V	Unit cell volume	(m³)
f	Friction factor	(–)	X, Y	Unknown coefficients	(–)
h	Heat transfer coefficient	(W/m²K)	ΔP	Pressure drop	(Pa)
k	Thermal conductivity	(W/kgK)	ΔT	Temperature drop	(K)
L	Unit cell length	(m)	ΔT_{LM}	Log-mean temperature drop	(K)
$\dot{m}$	Mass flow rate	(kg/s)	*Greek Letters*		
N	Polynomial order	(–)			
Nu	Nusselt number	(–)	η	Webb efficiency	(–)
P	Pressure	(Pa)	μ	Dynamic viscosity	(Pa-s)
$\dot{Q}$	Heat transfer rate	(W)	ρ	Density	(kg/m³)
Re	Reynolds number	(–)	ϕ	Fitted polynomial function	(–)

Subscript

avg	Average	LM	Log-mean
i	Indexing value	out	Out
in	In	w	Wall

REFERENCES

Ahn, Y., Bae, S. J., Kim, M., Cho, S. K., Baik, S., Lee, J. I., & Cha, J. E. (2015). Review of supercritical CO2 power cycle technology and current status of research and development. *Nuclear Engineering and Technology*, *47*(6), 647-661.

ANSYS, Inc. (2018a) *Ansys® Academic Research Mechanical, Release 18.0*.

ANSYS, Inc. (2018b) *Ansys® Academic Research Fluent, Release 18.0.*

Bergman, T. L., Incropera, F. P., DeWitt, D. P., & Lavine, A. S. (2011). *Fundamentals of heat and mass transfer* (7th ed.). Hoboken, NJ: John Wiley & Sons.

Cabeza, L. F., de Gracia, A., Fernández, A. I., & Farid, M. M. (2017). Supercritical CO2 as heat transfer fluid: A review. *Applied Thermal Engineering*, *125*, 799-810.

De Bock, H. P. J., & Gerstler, W. D. (2019). *U.S. Patent Application No. 16/219,540*.

Dittus, F. W. & Boelter, L. M. K. (1930). Heat Transfer in Automobile Radiators of the Tubular Type. *University of California Publications in Engineering 2*(13), 443-461.

Dostal, V. (2004). *A supercritical carbon dioxide cycle for next generation nuclear reactors* (Doctoral dissertation, Massachusetts Institute of Technology, Department of Nuclear Engineering).

Huang, Z., Hwang, Y., & Radermacher, R. (2017). Review of nature-inspired heat exchanger technology. *International Journal of Refrigeration*, *78*, 1-17.

Gerstler, W. D., & Erno, D. (2017). Introduction of an additively manufactured multi-furcating heat exchanger. In *16th IEEE Intersociety Conference on Thermal and Thermomechanical Phenomena in Electronic Systems (ITherm)* (624-633). IEEE.

Gerstler, W. D., Erno, D. J., Kenworthy, M. T., Rambo, J. D., & Sabo, N. K. (2016). *U.S. Patent Application No. 15/077,191*.

Gerstler, W. D., Erno, D. J., Kenworthy, M. T., Rambo, J. D., & Sabo, N. K. (2017). *E.U. Patent Application No. EP17162283.0A*.

Lemmon, E.W., Bell, I.H., Huber, M.L., & McLinden, M.O. (2013). NIST Standard Reference Database 23: Reference Fluid Thermodynamic and Transport Properties-REFPROP, Version 9.1, National Institute of Standards and Technology, Standard Reference Data Program, Gaithersburg, MD, USA.

Le Pierres, R., Southall, D., & Osborne, S. (2011). Impact of mechanical design issues on printed circuit heat exchangers. In *Proceedings of SCO2 Power Cycle Symposium*, 24-25.

Manglik, R. M., & Bergles, A. E. (1995). Heat transfer and pressure drop correlations for the rectangular offset strip fin compact heat exchanger. *Experimental Thermal and Fluid Science*, *10*(2), 171-180.

Meshram, A., Jaiswal, A. K., Khivsara, S. D., Ortega, J. D., Ho, C., Bapat, R., & Dutta, P. (2016). Modeling and analysis of a printed circuit heat exchanger for supercritical CO2 power cycle applications. *Applied Thermal Engineering*, *109*, 861-870.

Nikitin, K., Kato, Y., & Ngo, L. (2006). Printed circuit heat exchanger thermal–hydraulic performance in supercritical CO2 experimental loop. *International Journal of Refrigeration*, *29*(5), 807-814.

Private communications. (2019).

Serrano, I. P., Cantizano, A., Linares, J. I., & Moratilla, B. Y. (2014). Modeling and sizing of the heat exchangers of a new supercritical CO2 Brayton power cycle for energy conversion for fusion reactors. *Fusion Engineering and Design*, *89*(9-10), 1905-1908.

Shih, T. H., Zhu, J., & Lumley, J. L. (1994). A new Reynolds stress algebraic equation model. *Computer Methods in Applied Mechanics and Engineering, 125*(1-4), 287-302.

Span, R., & Wagner, W. (1996). A new equation of state for carbon dioxide covering the fluid region from the triple-point temperature to 1100 K at pressures up to 800 MPa. *Journal of Physical and Chemical Reference Data*, *25*(6), 1509-1596.

Webb, R. L., & Kim, N. Y. (2005). *Enhanced heat transfer* (2nd ed.). New York, USA: Taylor and Francis.

ACKNOWLEDGEMENT

The information, data, or work presented herein was funded in part by the Advanced Research Projects Agency-Energy (ARPA-E), U.S. Department of Energy, under Award Number DE-AR0001120, the Engie Chuck Edwards Memorial Fellowship, and the Modeling and Optimization Consortium at the University of Maryland. The views and opinions of authors expressed herein do not necessarily state or reflect those of the United States Government or any agency thereof.